35th Annual International Conference of the IEEE EMBS
Osaka, Japan, 3 - 7 July, 2013

Production of acoustic field with multiple focal points to control high amount of microbubbles in flow using a 2D array transducer*

Kohji Masuda, *Member, IEEE*, Naoto Hosaka, Ren Koda, Shinya Onogi and Takashi Mochizuki

***Abstract*— We have newly developed a 2D array transducer to control the behavior of microbubbles, which is different from that for HIFU therapy, to emit continuous wave by designing acoustic field including multiple focal points. In the experiment using a straight path model, we have confirmed that higher concentration of acoustic energy does not result more aggregation. We also have confirmed the trapped areas of microbubbles are located not in the peak of the distribution of sound pressure, but in the middle range. The dispersion of acoustic energy is important because there was a relation in the trapping performance of microbubbles and the shape of acoustic field.**

I. Introduction

Nowadays therapeutic applications using microbubbles under ultrasound exposure have been proposed, which are ultrasound thermal therapy [1] to improve the efficiency of high intensity focused ultrasound (HIFU) therapy, and physical drug delivery [2] to allow the uptake of larger molecules into cells. However, because of the diffusion of microbubbles in the human body, it is difficult to enhance the density of microbubbles near the desired target area. To control the local concentration of microbubbles, we have ever reported our attempts to control microbubbles using the primary and secondary acoustic forces to elucidate the conditions in sound pressure, central frequency of ultrasound, and flow velocity for active path selection [3,4] and trapping in blood flow [5] of microbubbles using artificial blood vessels. We had experimentally found that the microbubbles aggregations were propelled to the vessel wall by primary acoustic force, increasing their size according to the second acoustic force. By accumulating the local density of microbubbles, the therapeutic efficiency would be enhanced. Fig. 1 shows the concept of treatment using multiple acoustic forces and mictobubbles. Because there is the limitation where a catheter can be reached, microbubbles are injected near the narrowest bifurcation in the upstream, where there must be many microbubbles, which do not reach to the desired target area. If the behavior of the microbubbles could be physically controlled, the area of side effect caused by unwanted microbubbles would be decreased, which has a possibility to reduce the amount of not only microbubbles but also drug, in case of drug delivery.

In the previous experiments we have examined with single element transducers to produce focused or plane acoustic fields, by using concave or flat transducers, respectively. However, considering an in vivo application, there is a limitation to place multiple transducers on the body surface because of the possibility of interference between transducers. Furthermore, it is difficult to change focal area dynamically to produce local acoustic fields at a desired position using a single element transducer. Thus we considered that a matrix array transducer, which is mainly used in HIFU therapy, has a potential to control the behavior of microbubbles because not only the shape of acoustic field can be designed, but also multiple focal area can be produced and steered simultaneously by changing delay time in sound elements.

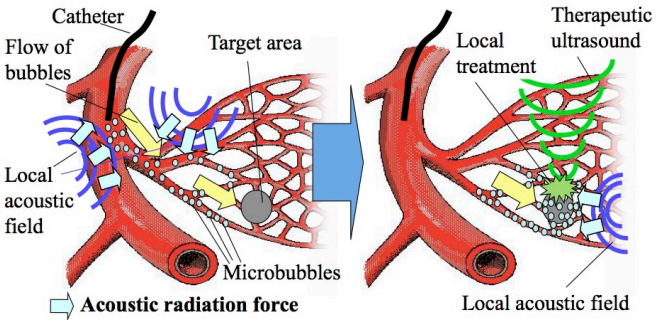

Figure 1. The concept of the treatment using miltiple acoistic forces and microbubbles.

Though the array transducer for HIFU therapy is normally constructed as a concave surface to concentrate higher energy to the focal area [6-8] by sacrificing steerable area of acoustic field, wider steerable area is important to control microbubbles. Furthermore, though a continuous wave is also necessary to guarantee acoustic force for active control of microbubbles in blood flow, the maximum sound pressure is required at least several hundred kPa, which is much less than that of HIFU therapy. Considering these reasons, we have newly developed a matrix array transducer with a flat surface to guarantee steerable area with the driving equipment to produce a continuous wave, where the waveform is different from HIFU therapy. In this paper, we report our challenge to produce an acoustic field of continuous wave to trap higher amount of microbubbles in flow.

II. Principle

We are going to confirm the distribution of acoustic field from the shape of microbubble aggregation propelled against vessel wall as shown in Fig. 2. By focusing continuous ultrasound in the middle of flow, the size of microbubbles aggregation is thought to be greater by involving microbubbles flown from upstream. To adjust the position

*Research supported by the Japan Society for the Promotion of Science (JSPS) through the Funding Program for Next Generation World-Leading Researchers (NEXT Program)..

Kohji Masuda, Naoto Hosaka, Ren Koda, Shinya Onogi and Takashi Mochizuki are with Graduate School of Bio-Applications and Systems Engineering, Tokyo University of Agriculture and Technology, Koganei, Tokyo, 184-8588 Japan (e-mail: masuda_k@cc.tuat.ac.jp).

and intensity of produced acoustic field, 2D array transducer was introduced and installed into our experiment.

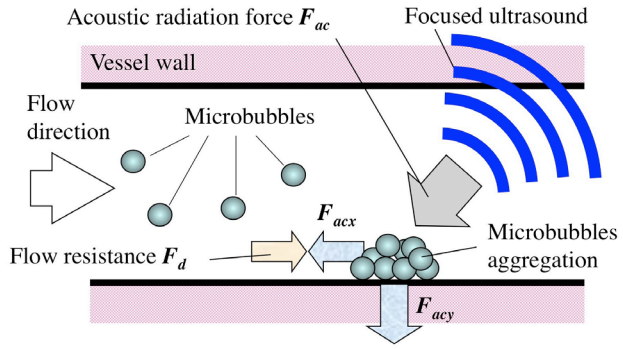

Figure 2. Acoustic force to trap microbubbles against vessel wall in flow.

Here we consider a flat 2D array transducer including N elements on the surface as shown in Fig. 3. When the focal point is determined as $F(x_F, y_F, z_F)$ in the transducer coordinate (x_T, y_T, z_T), and assuming the elements are allocated on $z_T = 0$ plane and the position of the elements are defined as (x_i, y_i, 0) (i = 1, N), the i-th element emits a sinusoidal acoustic wave with eq. (1).

$$E_i(t) = A \sin 2\pi f(t + \phi_i), \tag{1}$$

where A is the amplitude, f is the frequency, and ϕ_i indicates the delay time to be given by the following equation.

$$\phi_i = \frac{1}{c} \underset{j=1}{\overset{N}{Max}} \left\{ \sqrt{(x_j - x_F)^2 + (y_j - y_F)^2 + z_F^2} - \sqrt{(x_i - x_F)^2 + (y_i - y_F)^2 + z_F^2} \right\}, \tag{2}$$

where c indicates the sound velocity in the medium, and the function $Max\{\ \}$ is defined to select the maximum value through the index. Thus this function should return the longest distance between the focal point and the position of all N elements.

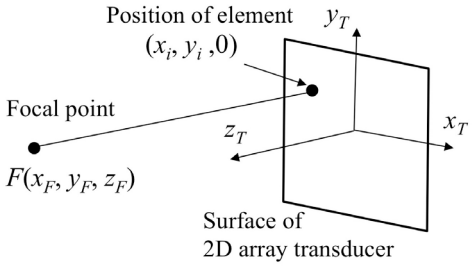

Figure 3. Position relationship between the 2D array transducet and the focal point.

To produce multiple focal points in the same time, it is possible to divide the elements into the same number of groups as the focal points and to apply similar delay times to elements in a group. However, the division of elements normally results the dispersion of sound energy. Thus the miltiple focal points can be produced by using all elements together. The i-th element can also emit an associated wave by summing sinusoidal waves as eq. (3) to produce multiple focal points F_m (m = 1, M).

$$E_i(t) = A \sum_{m=1}^{M} \sin 2\pi f(t + \phi_{i,m}), \tag{3}$$

where $\phi_{i,m}$ indicates the delay time for the focal point of F_m and calculated in the same way to eq. (2).

Finally the amplitudes and the delay times for the all elements are given through these equations to obtain a desired acoustic field.

III. Experiment

A. Experimental setup

We have used a square flat array transducer, which includes air-backed 64 PZT elements with the aperture of 23.9 x 23.9 mm^2, where the size of each element of 2.9 x 2.9 mm^2, and the pitch of the elements of 3.0 mm. The resonance frequency of the element is 1 MHz. The driving equipment produces continuous square wave with minimum delay pitch of 5 ns to obtain a sinusoidal wave from each element, where the reason why the square wave is applied to each element is to simplify the construction of the amplifier. Also because of the specific bandwidth on the elements, a narrowband continuous wave is emitted from the element. Fig. 1 shows the experimental setup. An artificial blood vessel (ABV), which was made of poly(ethylene glycol) [3-5] with the external size of 85 x 55 x 10 mm^3, was fixedly floated from the bottom of a water tank with filled water. We have prepared a straight path model as shown in Fig. 4. The shape of the cross section is circle with the diameter of 2 mm.

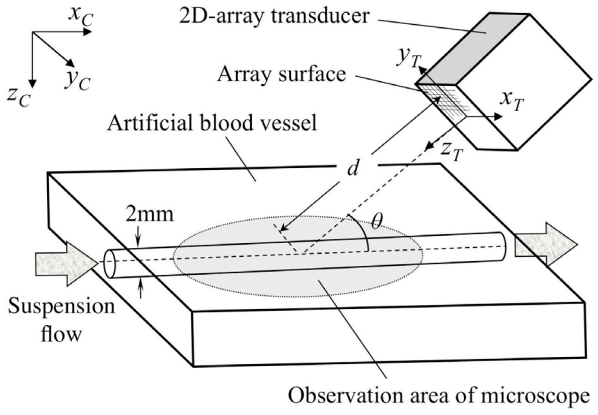

Figure 4. Schematic of the experiment with the artificial blood vessel, the transducer and the observation area.

The observation area can be focused and adjusted in the desired area in ABV by a high-speed camera 1024-PCI (Photoron) with an optical microscope CX5040SZ (HIROX) to observe the path through the transparent bottom plate of the tank. The source of light is located above the water tank. The axis of matrix array transducer was set to cross the center of the observation area with the angle θ and the distance d, where the array surface was entirely soaked below water. The whole view of the experimental setup is shown in Fig. 5. Also we prepared the suspension of microbubbles, which are F-04E microcapsules (Matsumoto Oil) [3,4] with a shell made of poly(vinyl chloride), a specific gravity of 0.0225, and an average diameter of 4 μm.

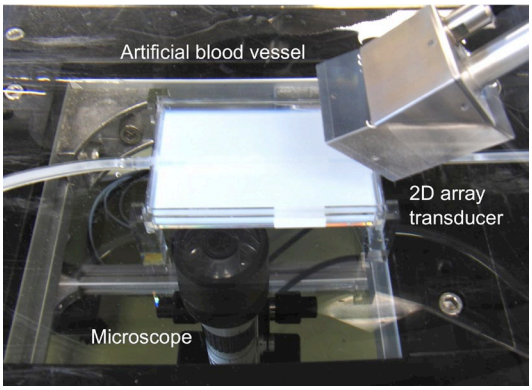

Figure 5. Configuration between transducer and the artificial blood vessel.

B. *Acoustic fields produced by array transducer*

Based on the calculation mentioned in the chapter 2, we designed the following three shapes of acoustic fields, which were produced by setting delay time in 64 elements individually. Figure 6 shows the calculated three-dimensional distribution of maximum sound pressure. The focused acoustic field is shown in Fig. 6 (a), where all of the elements contribute to make the focal point from the array surface at (x_T, y_T, z_T) = (0, 0, 50) [mm]. Here the distribution of sound pressure was obtained by the following procedures; First a normalized distribution of sound pressure was calculated. Then the array transducer was actually drived in water with an amplitude for each element to be 10 V-pp, which is the limitation of the transducer. The sound pressure of the focal point was directly measured by using a hydrophone to derive magnitude of sound pressure. In this case the maximum sound pressure in the focal point was 318 kPa-pp, which value is relatively converted to the normilized distribution and also to calculate the following other two acoustic fields.

Figs. 6 (b) and (c) indicate acoustic fields including two focal points, which were produced by dividing into two groups from the 64 elements to make their own focal points. The focal point of F_U for upper stream was focused by using 24 elements, where the focal point of F_L for lower stream was focused by using rest 40 elements. In Figs. 6 (b) and (c), the positions of the focal point of F_U were (-9, 0, 50) and (-9, 1, 50) [mm], respectively, in the coordinate (x_C, y_C, z_C). The position of F_L (3, 0, 50) was common.

C. *Evaluation of trapped area of microbubbles*

When the suspension of microbubbles was injected under continuous ultrasound emission, cloudy aggregations of microbubbles were observed in the middle of the ABV in the observation area, whereas no significant aggregations were observed in the case without ultrasound. To evaluate the trapped area of microbubbles quantitatively, which were considered to be sticking to the vessel wall, we calculated by processing successive microscopic images [5]. First the original image was converted to a gray scale image for application to unsharp masking for edge enhancement of the aggregations. Here, the brightness of the aggregations is clearly enhanced to distinguish them from thick suspension. Then, calculating the binary image by discriminant analysis method, the total trapped area of microbubbles is obtained.

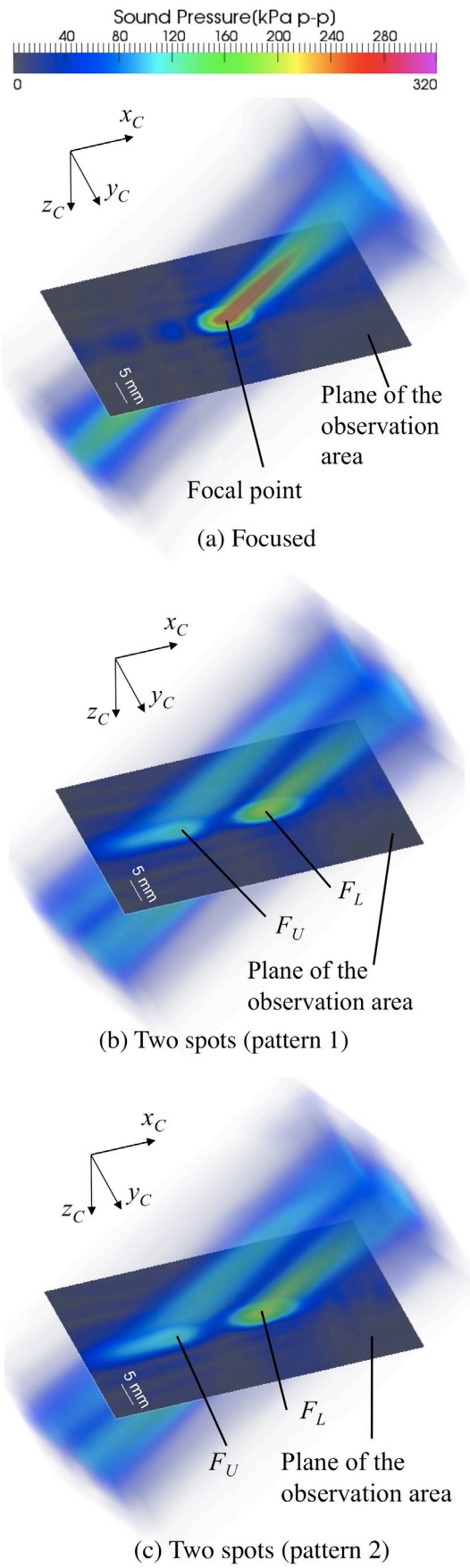

Figure 6. Three-dimensional distribution of maximum sound pressure.

IV. Results

We have applied to the straight path model of ABV under exposure of the acoustic field with Fig. 3 (a) focused, (b) two spots (pattern 1) and (c) two spots (pattern 2) to compare the trapping performance of microbubbles. The axis of matrix array transducer was set with the angle θ = 40˚ and the distance d = 50 mm in Fig. 4. Figure 7 shows the microscope images of the observation area 35 s after injection of the suspension under exposure of three kinds of acoustic fields, at a flow velocity of 20 mm/s from left to right, a microbubble concentration of 1.18 µl/ml, where the maximum acoustic intensity of 844 mW/cm^2 (SPTA) were same to the previous section.

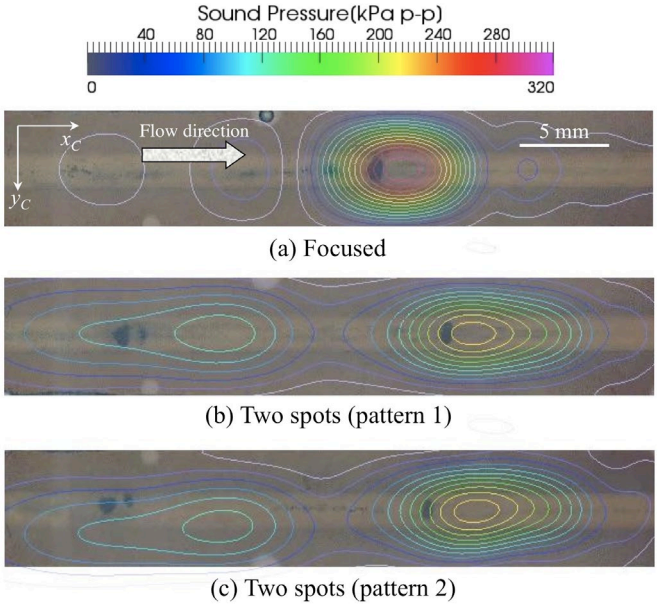

Figure 7. Microscope images of the observation area 35 s after injection under exposure of three shapes of acoustic field (flow velocity, 20 mm/s).

From the results in Fig. 7, most microbubbles were trapped in the upstream of the main peak. Comparing the focused and the two spots (pattern 1), though the trapped amount by main peak in the focused one was more than that of the two spots, the latter could trap by the sub peak located in upstream. To investigate the effect of the sub peak to the total trapped area, the positions of the sub peak in the pattern 2 was shifted 1 mm. Figure 8 shows time variation of the total trapped areas of microbubbles versus the three kinds of acoustic field, where the values were averaged from 5 attempts. In the pattern 2 the sub peak contribute to trap microbubbles less than the pattern 1 because it was apart from the straight path. As the result, total trapped area was increased in the two spots rather than the focused one, which indicates the spatial area of acoustic field passing through the path is dominant to the amount of trapped microbubbles.

We have also confirmed that the dispersion of acoustic energy on the path was important. Higher concentration of acoustic energy does not result more aggregation if there is an area limitation of flow. In the experiment, we have confirmed the trapped areas of microbubbles are located not in the peak of the distribution of sound pressure, but in the middle range. Thus it is required to derive the distribution of acoustic force to analyze and to control the behavior of microbubbles according to the flow condition.

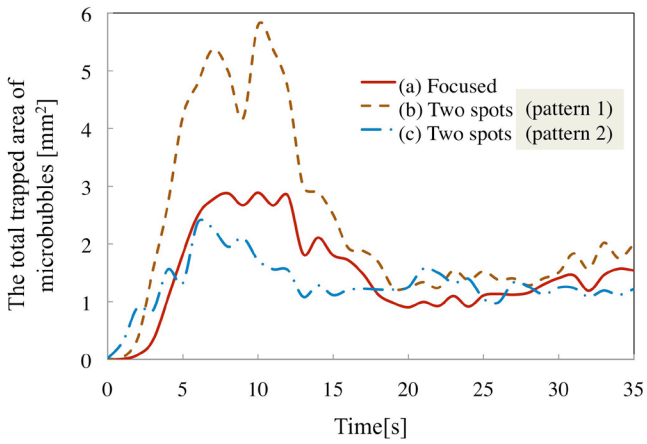

Figure 8. Time variation of total trapped area of microbubbles versus the four shapes of acoustic fields (flow velocity, 20 mm/s).

To apply to *in vivo* application, we consider that the following techniques are necessary; recognition technique of precise shape of blood vessel including the target area for treatment, and adjustment method of 2D array transducer to make focus to the desired blood vessel. We are already working with the other projects, which are a blood vessel network reconstruction [9], and a navigation system for ultrasound field positioning [10].

V. Conclusion

We have designed totally seven shapes of acoustic field to apply to trap microbubbles in flow using a matrix array transducer with 64 elements. We have confirmed that there is a relation in the trapping performance to the acoustic area in flow and concentration. In the next step we are going to measure quantitatively for precise evaluation to realize more appropriate shape of acoustic field.

References

[1] G. J. Liu, F. Moriyasu, T. Hirokawa, et al.: Ultrason. Med. Biol. **36** (2010) 78.

[2] N. Kudo, K. Okada, and K. Yamamoto: Biophys. J. **96** (2009) 4866.

[3] K. Masuda, Y. Muramatsu, S. Ueda, et al.: Jpn. J. Appl. Phys. **48** (2009) 07GK03.

[4] K. Masuda, N. Watarai, R. Nakamoto, and Y. Muramatsu: Jpn. J. Appl. Phys. **49** (2010) 07HF11.

[5] K. Masuda, R. Nakamoto, N. Watarai, et al.: Jpn. J. Appl. Phys. **50** (2011) 07HF11.

[6] K. Otsu, S. Yoshizawa, and S. Umemura: Jpn. J. Appl. Phys. **50** (2011) 07HC02.

[7] R. Matsuzawa, T. Shishitani, S. Yoshizawa, and S. Umemura: Jpn. J. Appl. Phys. **51** (2012) 07GF26.

[8] G. Y. Hou, J. Luo, F. Marquet, et al.: Ultrasound in Med. & Biol., **37** (2011) 2013.

[9] A. Bossard, T. Kato and K. Masuda: Proc. of IEEE EMBC (2012) pp. 5470-5473.

[10] S. Onogi, Y. Taguchi, Y. Sugano, et al.: Advanced Biomedical Engineering, **1** (2012) 16.